Flow Velocity Field in a Flame Submitted to Acoustic Modulations

S. Ducruix ‡, D. Durox, S. Candel
Laboratoire EM2C, CNRS and École Centrale Paris,
92295 Châtenay-Malabry, FRANCE
‡ e-mail : ducruix@em2c.ecp.fr

Key words : laminar premixed flame, acoustic-flame interactions, transfer function.

Coupling of acoustics and combustion may lead to instabilities in many practical devices. The determination of the flame transfer function is then essential to the understanding of the phenomena. In this respect, it is first natural to consider the case of a small scale burner before dealing with more complex systems.
In the present experiment, a driver unit, placed at the bottom of a conical flame burner, creates a periodic modulation of the velocity at the burner exit [1–3]. The frequency and amplitude of the acoustic modulation induce different responses of the flame. This configuration is used in [4] to determine the flame transfer function and compare it with an analytical model. The model relies on the relatively strong assumption that the fluctuating velocity in the fresh stream is uniform and that its radial component is negligible.
The aim of the present study is to measure the velocity field in the fresh gases and determine whether these assumptions are relevant and for what range of frequencies. The experimental setup is first described in section 1. The modeling of the transfer function is briefly underlined and a comparison with experimental results for a particular case is proposed in section 2. The velocity measurements are then described and the velocity evolution during acoustic cycles is finally investigated for different frequencies in section 3.

1 Experimental Setup

Experiments were carried out in the configuration shown in Fig.1.

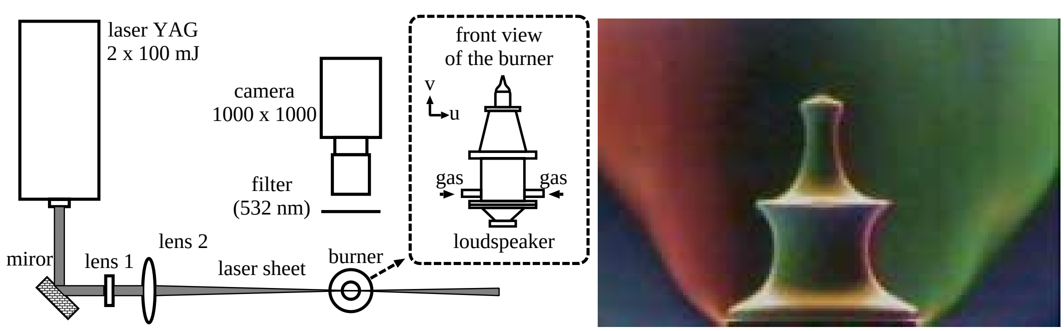

(a) Experimental setup (b) Instantaneous schlieren visualisation

Figure 1: Experiment characteristics: Φ = 1.05, v_0 = 0.97 m.s^{-1}, v_1 = 0.192 m.s^{-1}, f_{mod} = 75.5 Hz.

The burner consists of a converging nozzle of 22 mm exit diameter, followed by a cylindrical end piece 3 cm long. A cylindrical tube, 120 mm long, containing various grids and honeycombs to produce a laminar flow at the exit is placed upstream from the nozzle. A driver unit, fed by a synthesizer and an amplifier occupies the base of the burner.

Experiments were carried out with a methane-air mixture at a fixed equivalence ratio of 1.05, corresponding to a laminar burning velocity, S_L, of 0.39 m.s^{-1}. The space-averaged flow velocity is equal to 0.97 m.s^{-1}. Fig. 1 shows a typical instantaneous schlieren image obtained for a modulation frequency of 75.5 Hz. The shape of the perturbed flame depends on the frequency and the amplitude of the modulation. Gas velocities are measured by Particle Imaging Velocimetry (PIV) (Fig. 1 and 2). Oil droplets, with a mean diameter of 2.5 μm, were used to seed the flow. Heat release fluctuations are deduced from CH* emission measurements, using a photomultiplier (PM) coupled with a 431 nm CH*-filter (see details in [4]).

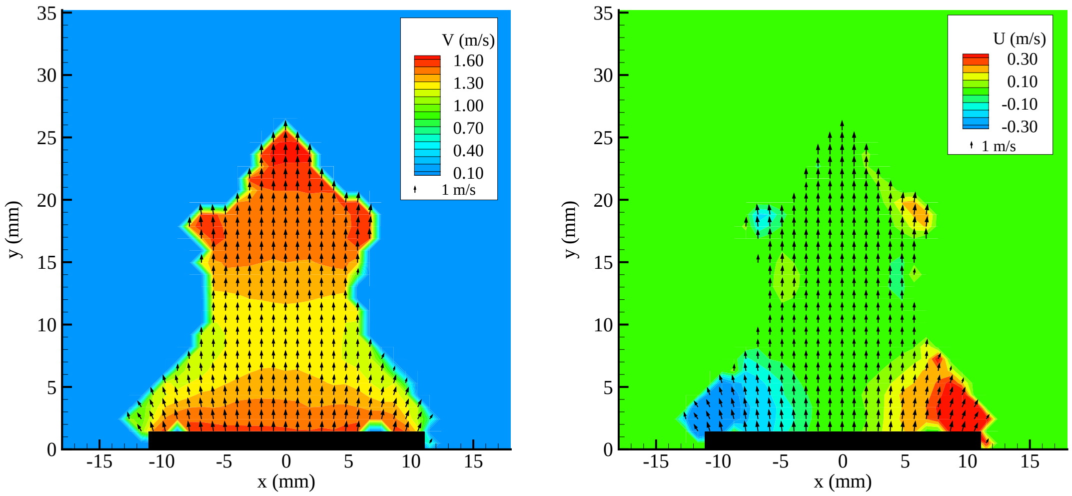

(a) Axial component

(b) Radial component

Figure 2: PIV measurements in the fresh gases, Φ = 1.05, v_0 = 0.97 m.s^{-1}, v_1 =0.192 m.s^{-1}, f_{mod} = 75.5 Hz. Arrows represent velocity vectors. Components of the velocity are superimposed.

2 Theoretical and Experimental Transfer Functions

The model described in this section is proposed in [4] and relies on a modified version of that devised in [5]. The main assumptions in the modeling concern the flow and flame velocities. The flame front is placed in a flow characterized by its mean and perturbation components (e.g. $v = v_0 + v_1$). The radial velocity u is supposed to be negligible, compared to the axial velocity v. The velocity field in the fresh gases is assumed to be axial and uniform, and one considers sinusoidal velocity modulations: $v_1 = v_1 \cos \omega t$. The burning velocity is assumed to be a constant and equal to the laminar burning velocity, S_L.

One can derive a relation between reduced heat release fluctuations, Q_1/Q_0 and velocity modulations v_1/v_0 at the burner outlet as a transfer function F characterized by its amplitude and phase [4]:

$$Q_1/Q_0 = v_1/v_0 |F(\omega_*)| \cos [\omega t - \phi(\omega_*)] \quad (1)$$

with

$$
\begin{aligned}
|F(\omega_*)| &= 2\left[(1-\cos\omega_*)^2 + (\omega_* - \sin\omega_*)^2\right]^{1/2}/\omega_*^2 \\
\phi(\omega_*) &= \tan^{-1}\left[(\omega_* - \sin\omega_*)/(1-\cos\omega_*)\right]
\end{aligned}
\tag{2}
$$

where ω_* is the reduced frequency: $\omega_* = \omega R/(S_L \cos\alpha_0)$ (where R is the burner radius, α_0 is the cone half-angle of the steady flame). As proposed in [5], it may also be interesting to approximate the transfer function as a first order system also characterized by its amplitude and phase:

$$
|H(w_*)| = \beta/\left(\beta^2 + \omega_*^2\right)^{1/2} \qquad \text{and} \qquad \psi(\omega_*) = \tan^{-1}\left(\omega_*/\beta\right)
\tag{3}
$$

β is a fitting parameter, estimated to be equal to 3. The amplitude and phase of the modeled transfer function

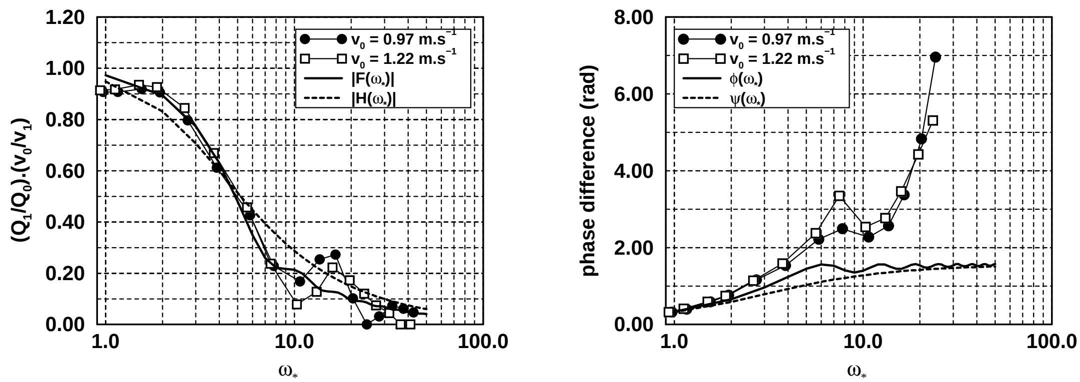

(a) (b)

Figure 3: Comparisons between analytical predictions and experimental results for the flame transfer function (a) amplitude and (b) phase. v_1 = 0.192 m.s^{-1}. Symbols indicates measurements for two mean velocities. The conversion factor K_c ($\omega_* = K_c f_{mod}$) is 0.194 for v_0 = 0.97 m.s^{-1} and 0.187 for v_0 = 1.22 m.s^{-1}.

are plotted as a function of ω_* and compared to experimental data in Fig. 3 (Q_1/Q_0 is the reduced r.m.s. PM intensity). For $\omega_* \leq 6$, the model and the first order approximation correctly predict the amplitude of the flame transfer function. For ω_* between 8 and 20, experimental results show that the amplitude of the transfer function increases to reach non-negligible values. This behavior is not predicted by both models. In all conditions, the phase difference increases with ω_* and values higher than 2π can be observed. In the corresponding range, analytical predictions, tending towards π/2, underestimate the flame response.

The limitations of the models are clearly apparent. It is now necessary to measure the velocity field in the fresh stream using PIV, in order to check the assumptions that are made in the modeling.

3 Determination of the Velocity Field

An example of an instantaneous velocity field in the fresh stream is given in Fig. 2 for a modulation frequency equal to 75.5 Hz (ω_* = 14.65). The axial and radial components of the velocity are superimposed. The non-uniformity of both components on the whole flame can be seen clearly.

In order to analyze the modifications of velocity fields with modulation frequency, velocity profiles are plotted in Fig. 4 and 5 during an acoustic cycle for two modulation frequencies. Fig. 4.(a) (resp. Fig. 5.(a)) describes the evolution of the axial component of velocity on the symmetry axis for f_{mod} = 10.5 Hz (resp. f_{mod} = 75.5 Hz). Fig. 4.(b) (resp. Fig. 5.(b)) presents the evolution of the radial component along x in a plane y = 1 mm above the burner exit for f_{mod} = 10.5 Hz (resp. f_{mod} = 75.5 Hz). Five instants in the acoustic cycle are represented.

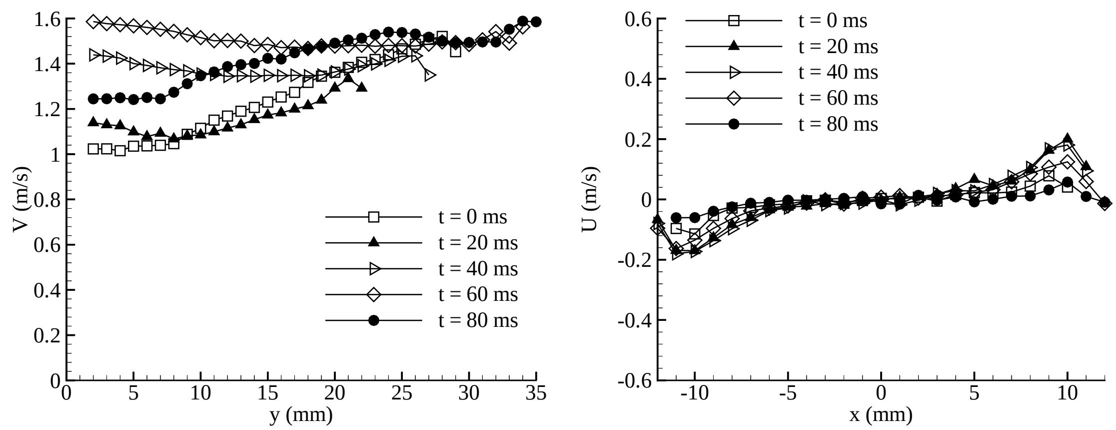

(a) Profiles of axial velocity along y, symmetry axis.

(b) Profiles of radial velocity along x (y = 1 mm).

Figure 4: Velocity profiles in the perturbed flame, frequency f_{mod} = 10.5 Hz (ω_* = 2.04).

Two different behaviors can be described. At low frequencies (ω_* = 2.04), Fig. 4.(a) shows a small and regular axial gradient at each instant of the acoustic cycle. The axial component of velocity varies between 1 and 1.6 m.s^{-1}. At a given instant in time, the axial gradient is almost uniform or varies slowly in the whole flame. The gradient is small and negative for large values of the ejection velocity in the exit plane and larger and positive for small values of the ejection velocity, except for the shortest flame length (t = 20 ms) when the gradient is less regular. The maximum gradient value is about 20 s^{-1}.
For this low frequency, the radial velocity remains small during the entire cycle (Fig. 4.(b)). The maximum value is 0.2 m.s^{-1}, corresponding to less than 15% of the mean axial velocity. Maximum values are encountered in the exit plane, near the edge of the burner. For the chosen instants, the radial component is always towards the burnt gases. Velocity vectors are almost axial in the flame. It can be seen in Fig. 4.(a) that the flame height changes significantly during an acoustic cycle, from 23 to 35 cm. This corresponds to variations in the heat release integrated on the whole flame, resulting in a high amplitude of the transfer function (Fig 3.(a)).

For higher frequencies (ω_* = 14.65), the space time evolution of the velocity is different (Fig. 5). The axial component presents a strong gradient on the axis near the exit plane, up to 30 s^{-1}. The axial gradient is then very small in the second part of the flame and the axial velocity is constant close to 1.3 m.s^{-1}. During part of the acoustic cycle, the axial component of the velocity depends only on y, as in the case of a low frequency modulation. During the other part of the cycle, the flame presents zones in which the axial component is higher on the edge of the flame than near the axis for a given y. These regions correspond to the convection of the modulation towards the top of the flame (Fig. 2). In contrast with the first case, the flame height is not greatly modified during an acoustic cycle. Perturbations wrinkle the flame front locally, but the global heat release is merely modified, corresponding to a small amplitude of the transfer function.
In this case, radial velocities are large in the exit plane and similar large values are found in other regions as

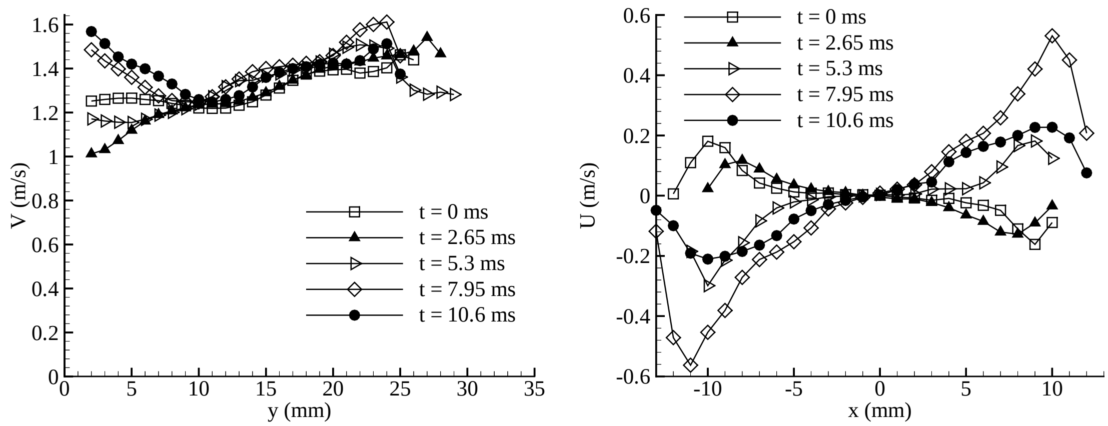

(a) Profiles of axial velocity along y, symmetry axis.

(b) Profiles of radial velocity along x (y = 1 mm).

Figure 5: Velocity profiles in the perturbed flame, frequency $f_{mod} = 75.5$ Hz ($\omega_* = 14.65$).

well. Fig. 5.(b) indicates that the radial velocity can reach values up to 0.6 m.s^{-1} near the exit, corresponding to 43% of the mean axial component. The radial component is oriented towards the burnt gases for part of the acoustic cycle and towards the symmetry axis for other instants.

Conclusion

Data obtained here with PIV are used to check the validity of assumptions made in the modeling. The velocity field in the fresh gases was assumed to be axial and uniform. The model assumptions may probably be acceptable for slightly wrinkled flames, with a small radial component of the velocity field. The axial component of velocity varies slowly and the radial component can be neglected. In this case, the flame responds as if it was completely stretched and compressed by the modulation, remaining globally conical. This justifies the assumptions made in the theoretical modeling. In contrast, these assumptions are too strong for larger reduced frequencies to correctly represent the acoustic-flame interactions. In this frequency range, velocity fields in the fresh stream show important gradients and a radial flow exists near the burner exhaust. The phase between heat release and velocity modulations is not well predicted. An improved model should take these features into account. One possible way would be to model the convection time for the perturbations, through a phase difference appearing in the velocity in the fresh gases.

References

[1] G. De Sœte. *Revue de l'I.F.P. et Annales des Combustibles Liquides*, 19:766–785, 1964.

[2] F. Baillot, D. Durox, and R. Prud'Homme. *Combust. Flame*, 88:149–168, 1992.

[3] D. Durox, S. Ducruix, and F. Baillot. *Proc. Combust. Inst.*, 27:883–889, 1998.

[4] S. Ducruix, D. Durox, and S. Candel. *Proc. Combust. Inst.*, 28, 2000.

[5] M. Fleifil, A.M. Annaswamy, Z.A. Ghoneim, and A.F. Ghoniem. *Combust. Flame*, 106:487–510, 1996.